

# Wide-range optical spectra of carbon nanotubes: a comparative study

K. Kamarás<sup>1,\*</sup>, Á. Pekker<sup>1</sup>, M. Bruckner<sup>1</sup>, F. Borondics<sup>1</sup>, A. G. Rinzler<sup>2</sup>, D. B. Tanner<sup>2</sup>, M. E. Itkis<sup>3</sup>, R. C. Haddon<sup>3</sup>, Y. Tan<sup>4</sup>, and D. E. Resasco<sup>4</sup>

<sup>1</sup> Research Institute for Solid State Physics and Optics, Hungarian Academy of Sciences, P.O. Box 49, 1525 Budapest, Hungary

<sup>2</sup> Department of Physics, University of Florida, Gainesville, FL 32611, USA

<sup>3</sup> Center for Nanoscale Science and Engineering, Departments of Chemistry and Chemical and Environmental Engineering, University of California, Riverside, CA 92521-0403, USA

<sup>4</sup> Department of Chemical, Biological, and Materials Engineering, University of Oklahoma, 100 East Boyd St, Norman, OK 73019, USA

Received 15 May 2008, accepted 27 June 2008

Published online 3 September 2008

PACS 78.30.Na, 78.40.Ri

\* Corresponding author: e-mail kamaras@szfki.hu

We present optical spectra from the far infrared through the ultraviolet spectral region of freestanding transparent carbon nanotube films: single-, double- and multiwalled, and containing varying amounts of tubes of different chirality. By comparing the spectral features in the far infrared and the near infrared/visible, we can estimate the

metallic/semiconducting content. We show by spectroscopic methods that doping the tubes increases both the conductivity and the transparency for visible light. We also discuss the influence of sample preparation and subsequent treatment on application possibilities.

© 2008 WILEY-VCH Verlag GmbH & Co. KGaA, Weinheim

**1 Introduction** Optical spectroscopy is one of the most widely used methods in characterization of carbon nanotubes. Recently, it was demonstrated that absorption and especially fluorescence studies can detect individual nanotubes and identify them by chirality index [1]. Most studies concentrated on the NIR/VIS spectral range where transitions between Van Hove singularities occur: based on these observations, selectivity by semiconducting/metallic character was reported both for ionic doping [2,3] and covalent functionalization [4]. Relatively less attention was devoted to the low-frequency part of the spectrum. Here we want to emphasize the importance of far-infrared measurements as a sensitive indicator of intrinsic charge carriers in metallic tubes and extrinsic carriers in doped materials.

**2 Experimental** Six types of tubes were used for this study: four were single-walled, one double-walled and one multiwalled. Single-walled laser-ablated nanotubes were produced by Tubes@Rice, arc-derived ones by Carbon Solutions, Inc. HiPCO tubes were commercial samples from CNi Nanotechnologies and two types of CoMoCat sam-

ples, commercial grade and research grade, from Southwest NanoTechnologies. Based on the average diameter, we divide the single-walled samples into small- and large-diameter groups (see Table 1). The width of the diameter distribution, though, is also varying among the families: HiPCO has the widest distribution, and the two CoMoCat samples differ in the content of metallic tubes, SG grade having a narrower distribution and consisting almost exclusively of semiconducting tubes. Double- and multiwall tubes were commercial products by Nanocyl SA.

All measurements were done on freestanding films, prepared according to Ref. [5] from nanotube suspensions in Triton-X, filtered on a mixed cellulose ester filter which was subsequently dissolved in acetone and the nanotube films captured on graphite frames. Films of thickness 300–400 nm were produced in this way, still thin enough to be transparent throughout the whole spectral range. The films were annealed in vacuum at 200 °C for two hours before measurement; this step is important in order to remove accidental doping by the chemicals used for purification [6]

**Table 1** Summary of the samples investigated

| Sample        | Origin                     | Average diameter (nm) |
|---------------|----------------------------|-----------------------|
| Arc           | Carbon Solutions           | 1.4                   |
| Laser         | Tubes@Rice                 | 1.3                   |
| HiPCO         | CNI Nanotechnologies       | 0.7                   |
| CoMoCat CG    | Southwest Nanotechnologies | 1.0 ± 0.3             |
| CoMoCat SG    | Southwest Nanotechnologies | 0.7                   |
| Double-Walled | Nanocyl                    | 2-3 (outer)           |
| Multi-Walled  | Nanocyl                    |                       |

and thereby allowing the comparison of pristine nanotubes without doping effects.

Several spectrometers were used, covering the full optical range from the far infrared through the ultraviolet: two Fourier-transform interferometers (Bruker 66v/S in the FIR/MIR, Bruker Tensor 28 in the MIR/NIR) and a JASCO grating instrument as well as an Ocean Optics fiber-optic spectrometer in the VIS/UV. Spectra were taken in transmission mode. Doping studies were conducted in a 10 cm gas cell with KBr windows. We converted the transmission to optical density (OD) by simply taking  $-\log T$ . This procedure neglects reflectance corrections and is therefore not fully quantitative, especially in the far infrared [7], however, the resulting OD value is monotonous with concentration, albeit not linear. This means that although we cannot use this procedure for estimating the metallic to semiconducting tube ratio, we can establish an order of the samples according to both dc conductivity and IR/VIS transmittance. A more detailed analysis of the optical constants, combining spectroscopy with thickness measurements by atomic force microscopy, will be presented in a forthcoming publication.

### 3 Results and discussion

**3.1 Undoped films** Figure 1 shows the optical density of all six samples investigated. In single-walled tubes, three typical features can be distinguished: 1. a low-frequency absorption, either peaked around  $100\text{ cm}^{-1}$  or increasing smoothly towards zero; 2. distinct peaks in the NIR/VIS range, corresponding to transitions between Van Hove singularities in the density of states; 3. a broad absorption peaking in the UV, caused by  $\pi \rightarrow \pi^*$  excitations of the entire  $\pi$ -electron system. Between regions 1 and 2 the absorption is low and this region constitutes the transparency window, important for applications.

It is apparent by comparing Figs. 1a and 1b that the small-diameter tubes used in this study consist of fewer types of nanotubes than the large-diameter ones, and that probably the metal/semiconducting ratio is also different between these samples. The structured appearance of the  $S_{11}$  transition in HiPCO as well as the extreme small width of this peak in scientific grade CoMoCat indicates that the distribution is not continuous as in the laser and arc samples.

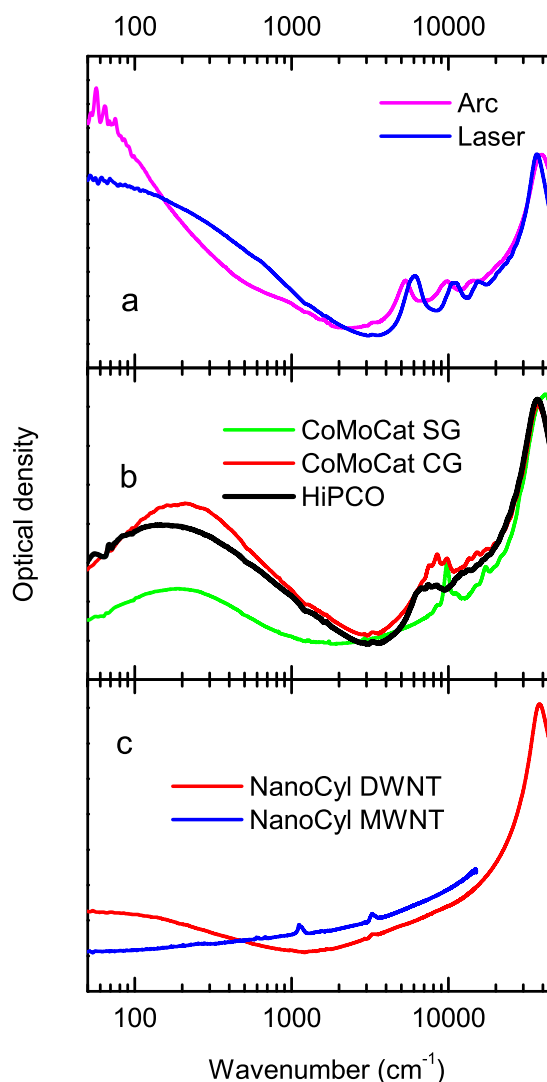


**Figure 1** Optical density of three types of carbon nanotubes: a) large diameter (arc and laser), b) small diameter (HiPCO and CoMoCat) and c) double-walled and multiwalled. Spectra are scaled at the  $\pi \rightarrow \pi^*$  peak.

Moreover, the difference between commercial and scientific grade CoMoCat samples manifests itself in both the narrowing of the  $S_{11}$  transition and the decrease in intensity of the low-frequency peak, indicating that the SG material contains not only a narrower distribution of semiconducting tubes, but the ratio of semiconducting to metallic tubes has also increased. Estimations of metal content in CoMoCat tubes vary considerably in the literature from 10 per cent [8] to 25 per cent [9]; according to the data presented here, the metal content of the CG type is close to HiPCO, whereas that of the SG type is less.

All three small-diameter samples show a distinct peak around  $100\text{ cm}^{-1}$ , in contrast to the large-diameter types,

which rather show a Drude-like absorption at low frequencies. Such low-frequency peaks are commonly seen in nanotube networks [6, 10] and have been interpreted in different ways, including simple geometrical effects [11]. The outspoken difference in this case rather points to an intrinsic origin of this peak, since the aspect ratio does not differ so much between samples as to cause this kind of variation. We believe that the small-diameter tubes, having fewer types of tubes by chirality overall, contain less armchair tubes relative to others [8], and thus the low-frequency curvature gap is better visible.

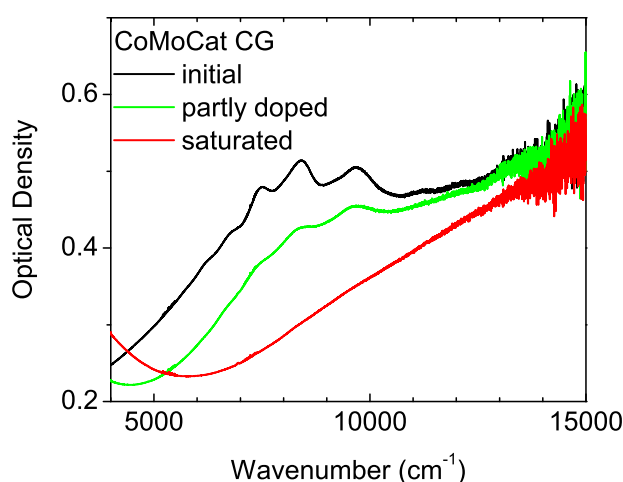


**Figure 2** Optical density of CoMoCat SG nanotubes before doping with  $\text{HNO}_3$  vapor and at saturation, in the spectral range of the first semiconducting transition. The optical density decreases and the peaks connected to the Van Hove singularities disappear, causing an overall lower and less structured optical density, i.e. higher transmission.

**3.2 Effects of doping** To study the effects of doping, we chose CoMoCat CG material because it contains few enough specimens to follow them individually, yet many enough to observe the effect of doping on several types of tubes. We followed the evolution of the spectra in the  $S_{11}$  region after exposing the film to nitric acid vapor. Nitric acid causes hole doping, similar to intercalated graphite [12]. The process arrived at saturation within five minutes. In Fig. 2, we show typical spectra: before and during doping and after saturation. Changes consist of the disappearance of all interband transitions, and the appearance of a low-frequency absorption which we assign to free-carrier excitations connected with the emptying of the occupied states through hole doping by the acid. This treatment increases the dc conductivity and the free-carrier absorption, thereby distorting the apparent metal/semiconductor ratio; this is the reason why before comparing spectroscopic features, all samples have

to undergo thermal treatment in order to remove spurious dopants.

**3.3 Connection to applications** The principal area in applications of transparent carbon nanotube films is that of transparent conducting coatings [13]. These applications require a wide spectral range of transparency, preferably between the infrared and the visible, and high dc conductivity, i.e. large optical conductivity (high optical density) in the far infrared [14]. From the above, it is clear that carbon nanotubes can fulfil both requirements; moreover, both the dc conductivity and the transparency range can be tuned by selecting the appropriate kind of tubes. The value of the transmission can be then adjusted by varying the thickness of the layer.

From the rather limited selection presented above, we can deduct some trends which influence the properties of potential conducting layers.

The far-infrared optical density scales with the dc conductivity of the material, while the transparency in the MIR to visible range grows with decreasing optical density. Thus, the ideal case for conducting electrodes is high optical density at the lowest frequencies and low optical density in a preferably wide frequency range, which, in case of solar energy applications, should include the visible region. Within these limits, the type of nanotube to be used depends very much on the particular application. From Fig. 1, it is clear that arc or laser material are recommended if high dc conductivity is desired, but their window of transparency is narrower than that of HiPCO or CoMoCat. The window of transparency for all materials lies at lower frequencies than ITO as shown in Fig. 3, but improvement can be achieved by doping, which reduces the interband transitions and widens the window (Fig. 2).

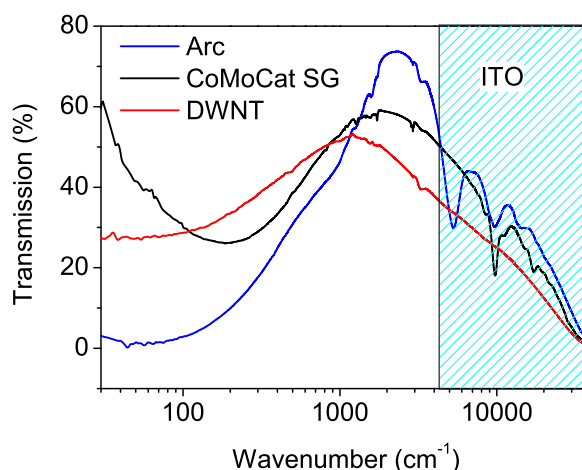


**Figure 3** Transmittance of three types of nanotubes in the spectral range investigated. The shaded area represents the application range of ITO.

Double-walled nanotubes comprise an interesting class in themselves: although their far-infrared absorbance is lower than that of single-walled ones, it is still high enough to achieve conductance and the range of transparency is the broadest among the samples investigated. Part of the reason why the absolute transmittance is lower than in single-walled tubes is that the mechanical properties are worse than in case of single-walled tubes, therefore only thicker films will be freestanding; however, most applications work in a limited frequency range and therefore can use an appropriate substrate to give mechanical support.

**4 Conclusions** We have presented wide-range optical spectra of freestanding carbon nanotube films. From these data we can characterize various nanotube types by conductivity and transparency, the most important parameters of coating applications. We showed that laser or arc material is optimal when high conductivity is desired, HiPCO and CoMoCat show a wider transparency region, and double-wall tubes exhibit the least structure in transmission. The latter effect, loss of structure with increasing transparency, can also be achieved by doping. These possibilities (tunable conductivity and transparency window) make carbon nanotubes feasible alternatives to conducting transparent oxides.

**Acknowledgements** Work in Hungary supported by the Hungarian National Research Fund (OTKA T049338) and by the European Commission (FP6 STREP project NEURONANO NMP4-CT-2006-031847). Work at Florida supported by the NSF, DMR-0305043, and the DOE, DE-AI02-03ER46070.

## References

- [1] S. M. Bachilo, M. S. Strano, C. Kittrell, R. H. Hauge, R. E. Smalley, and R. B. Weissman, *Science* **298**, 2361 (2002).
- [2] S. Kazaoui, N. Minami, R. Jacquemin, H. Kataura, and Y. Achiba, *Phys. Rev. B* **60**, 13339 (1999).
- [3] F. Hennrich, R. Wellmann, S. Malik, S. Lebedkin, and M. M. Kappes, *Phys. Chem. Chem. Phys.* **5**, 178 (2003).
- [4] M. S. Strano, C. A. Dyke, M. L. Usrey, P. W. Barone, M. J. Allen, H. Shan, C. Kittrell, R. H. Hauge, J. M. Tour, and R. E. Smalley, *Science* **301**, 1519 (2003).
- [5] Z. Wu, Z. Chen, X. Du, J. Logan, J. Sippel, M. Nikolou, K. Kamarás, J. R. Reynolds, D. B. Tanner, A. F. Hebard, and A. G. Rinzler, *Science* **305**, 1273 (2004).
- [6] F. Borondics, K. Kamarás, M. Nikolou, D. B. Tanner, Z. Chen, and A. G. Rinzler, *Phys. Rev. B* **74**, 045431 (2006).
- [7] Á. Pekker, F. Borondics, K. Kamarás, A. G. Rinzler, and D. B. Tanner, *phys. stat. sol. (b)* **243**, 3485 (2006).
- [8] A. Jorio, A. P. Santos, H. B. Ribeiro, C. Fantini, M. Souza, J. P. M. Vieira, C. A. Furtado, J. Jiang, R. Saito, L. Balzano, D. E. Resasco, and M. A. Pimenta, *Phys. Rev. B* **72**, 075207 (2005).
- [9] G. Lolli, L. Zhang, L. Balzano, N. Sakulchaicharoen, Y. Tan, and D. E. Resasco, *J. Phys. Chem. B* **110**, 2108 (2006).
- [10] M. E. Itkis, D. E. Perea, S. Niyogi, S. M. Rickard, M. A. Hamon, H. Hu, B. Zhao, and R. C. Haddon, *Nano Lett.* **3**, 309 (2003).
- [11] N. Akima, Y. Iwasa, S. Brown, A. M. Barbour, J. Cao, J. L. Musfeldt, H. Matsui, N. Toyota, M. Shiraishi, H. Shimoda, and O. Zhou, *Adv. Mater.* **18**, 1166 (2006).
- [12] A. R. Ubbelohde, *Proc. Roy. Soc. London Ser. A* **304**, 25 (1968).
- [13] K. Lee, Z. Wu, Z. Chen, F. Ren, S. J. Pearton, and A. G. Rinzler, *Nano Lett.* **4**, 911 (2004).
- [14] L. Hu, D. S. Hecht, and G. Grüner, *Nano Lett.* **4**, 2513 (2004).